PROCEEDINGS OF SPIE

SPIEDigitalLibrary.org/conference-proceedings-of-spie

The ERIS adaptive optics system: from design to hardware

Riccardi, A., Esposito, S., Agapito, G., Biliotti, V., Briguglio, R., et al.

A. Riccardi, S. Esposito, G. Agapito, V. Biliotti, R. Briguglio, L. Carbonaro, G. Di Rico, D. Ferruzzi, C. Giordano, P. Grani, T. Mazzoni, A. Puglisi, M. Xompero, M. Bonaglia, A. Baruffolo, M. Kasper, R. J. Dorn, D. Barr, M. Downing, J. Reyes, C. Soenke, M. Suárez Valles, "The ERIS adaptive optics system: from design to hardware," Proc. SPIE 10703, Adaptive Optics Systems VI, 1070303 (10 July 2018); doi: 10.1117/12.2309869

SPIE.

Event: SPIE Astronomical Telescopes + Instrumentation, 2018, Austin, Texas, United States

The ERIS Adaptive Optics System: from design to hardware

A. Riccardi*[a,d], S. Esposito[a,d], G. Agapito[a,d], V. Biliotti[a,d], R. Briguglio[a,d], L. Carbonaro[a,d], G. Di Rico[b,d], D. Ferruzzi[a,d], C. Giordano[a,d], P. Grani[a,d], T. Mazzoni[a,d], A. Puglisi[a,d], M. Xompero[a,d], M. Bonaglia[a,d], A. Baruffolo[c], M. Kasper[e], R. J. Dorn[e], D. Barr[e], M. Downing[e], J. Reyes[e], C. Soenke[e], M. Suárez Valles[e]

[a]INAF-Osservatorio Astrofisico di Arcetri, Largo E. Fermi 5, 50125 Firenze, Italy
[b]INAF-Osservatorio Astronomico d'Abruzzo, Via Mentore Maggini, 64100 Teramo, TE, Italy
[c]INAF-Osservatorio Astronomico di Padova, Vicolo dell'Osservatorio, 5, 35141 Padova PD, Italy
[d]ADONI – Laboratorio Nazionale di Ottica Adattiva, Italy
[e]European Southern Observatory, Karl-Schwarzschild-Strasse 2, D-85748 Garching, Germany

ABSTRACT

ERIS is the new AO instrument for VLT-UT4 led by a Consortium of Max-Planck Institut fuer Extraterrestrische Physik, UK-ATC, ETH-Zurich, NOVA-Leiden, ESO and INAF. The ERIS AO system provides NGS mode to deliver high contrast correction and LGS mode to extend high Strehl performance to large sky coverage. The AO module includes NGS and LGS wavefront sensors and, with VLT-AOF Deformable Secondary Mirror and Laser Facility, will provide AO correction to the high resolution coronagraphic imager NIX (1-5um) and the IFU spectrograph SPIFFIER (1-2.5um). In this paper, we present the final design of the ERIS AO system and the status of the of current MAIV phase.

Keywords: ERIS, VLT, Wavefront Sensing, Deformable Secondary Mirror, Adaptive Optics System, SPARTA, CCD220, Laser Guide Star

1. INTRODUCTION

ERIS, the Enhanced Resolution Imager and Spectrograph[1], is a new 1-5 μm instrument for the Cassegrain focus of the UT4/VLT telescope that is equipped with the Adaptive Optics Facility (AOF)[2][3]. The instrument is led by a Consortium of Max-Planck Institut für Extraterrestrische Physik (MPE, leading institute), UK Astronomy Technology Centre (UK-ATC), Institute for Particle Physics and Astrophysics (ETH-Zurich), NOVA (Leiden Observatory), European Southern Observatory (ESO) and Istituto Nazionale di Astrofisica (INAF Arcetri, Abruzzo and Padova). The ERIS Consortium have taken the lead of the project in early 2015, passed the Preliminary Design Review (PDR)[4] in February 2016 and the Final Design Review the end of May 2017. The project is currently in Manufacturing, Assembly, Integration and Verification (MAIV) phase. The present paper reports the design of the ERIS AO sub-system as result of the FDR and the status of the MAIV. For more information on ERIS at the full instrument level, refer to [1].

The instrument is made of the following sub-systems (see Figure 1):

- two science instruments, which receive their light via a IR/VIS dichroic beam-splitter located in the AO module.
    - NIX[5][6][7][8] provides diffraction limited imaging, sparse aperture masking (SAM) and pupil plane coronagraphy capabilities from 1-5 μm (i.e. J-M'), either in "standard" observing mode or with "pupil tracking" and "burst" (or "cube") readout mode. NIX is a cryogenic instrument and it is equipped with a 2048 × 2048 detector providing a field of view of 53" x 53"
    - SPIFFIER[1][9] is an upgraded version of SPIFFI, the 1-2.5 μm integral field unit used on-board SINFONI, that will be modified to be integrated into ERIS. Its observing modes are identical to those of SINFONI, with the addition of a high-resolution mode.
    - The two science instruments do not operate simultaneously, an insertable mirror behind the IR/VIS dichroic allows to select the instrument.
- the AO module has wavefront sensing and real-time computing capabilities. It interfaces to the AOF infrastructure and it is required to provide the following observing modes:

Adaptive Optics Systems VI, edited by Laird M. Close, Laura Schreiber, Dirk Schmidt, Proc. of SPIE Vol. 10703, 1070303 · © 2018 SPIE
CCC code: 0277-786X/18/$18 · doi: 10.1117/12.2309869

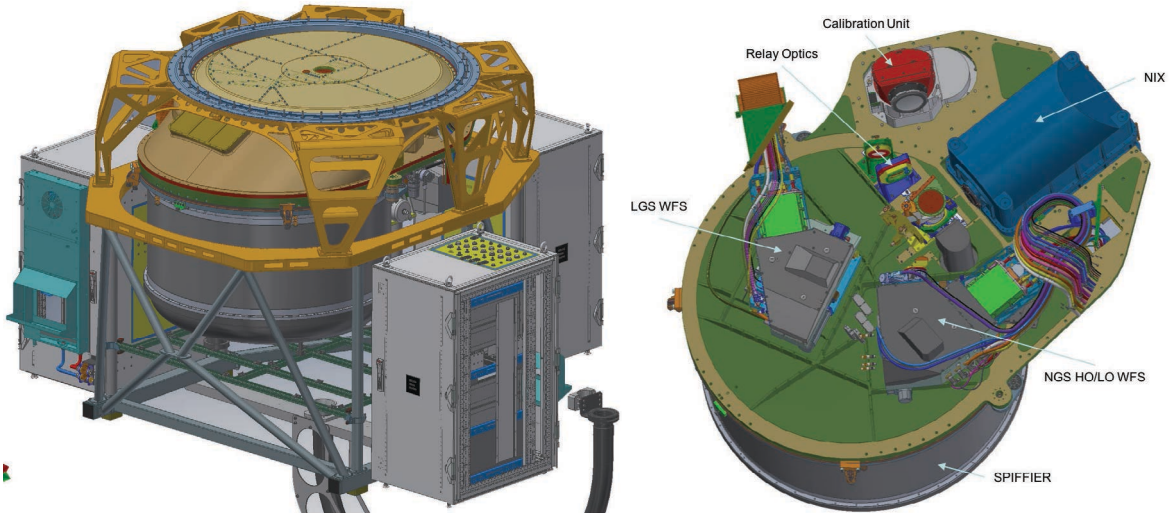

Figure 1 Left: the ERIS instrument. Right: the ERIS sub-systems (optical bench internal view).

- LGS-mode: a Wavefront Sensor (WFS) provides high-order AO correction using a Laser Guide Star (LGS) on-axis and a second WFS provides low-order correction and truth sensing using a Natural Guide Star (NGS) in the patrol field (R≤1arcmin).
- NGS-mode: a WFS provides high-order AO correction using a NGS in the patrol field;
- Seeing Enhanced mode: only the on-axis LGS WFS is used for the high-order correction. This mode is used when no suitable NGS is available for the AO fast correction of the tip-tilt, relaying to the Field Stabilization function of the telescope for tracking and wind buffeting correction using a NGS in the Active Optics field.

- The Calibration Unit (CU)[10], which provides facilities to calibrate the scientific instruments (remove instrument signature) and perform troubleshooting and periodic maintenance tests of the AO modules.

The ERIS AO concept maximizes the re-use of existing AOF sub-systems and components as explicitly requested by the ERIS Top Level Requirements (TLRs). In particular, the AO correction is provided by the AOF Deformable Secondary Mirror (DSM)[2][11] and the artificial sodium LGS is generated by one of the launchers of the 4LGSF system[12]. Moreover the ERIS AO sub-system uses components from the AOF GLAO and LTAO systems (GALACSI and GRAAL), namely the wavefront sensor camera detectors (EMCCD220) and a modified version of SPARTA/AOF as Real-Time Computer (RTC).

For a description of the AO control electronics architecture refer to [13]; for the ERIS software refer to [14].

2. LAYOUT

Figure 2 shows the conceptual scheme of the ERIS instrument, including the Adaptive Optics (AO) sub-system (or module). The set of optical components, that relays the telescope optical beam out from the Cassegrain Flange to the science instruments and to the AO WFSs, is defined as Warm Optics (WO) and is considered part of the AO sub-system (see Figure 3).

The ERIS instrument is installed at the UT4/VLT Cassegrain Focal Station. The beam from the telescope is split by a 45deg IR/VIS dichroic, transmitting the IR (1-5μm) light to the science instruments and the visible (<1μm) to the AO WFSs. The IR/VIS dichroic is the first component of the WO and has also the practical function of decoupling the alignment of the AO beam from the science beam. The size of the dichroic (100x144 mm^2) is constrained by the reflected AO patrol field of 2 arcmin diameter. In order to avoid ambient thermal background being injected in the science instrument by the back surface of the dichroic, a LN2 cold plate is facing on the back of the dichroic from an extension of the SPIFFIER cryostat.

The two instruments (SPIFFIER and NIX) are simultaneously integrated in ERIS. SPIFFIER receives directly the beam from the IR/VIS dichroic. NIX is fed by inserting a 45deg gold-coated mirror, the NIX Selector Mirror, still part of the WO. The mirror mount, when deployed, is preloaded by the stage to a mechanical stop to reduce flexures when changing the gravity vector.

The AO module does not need to internally integrate any deformable mirror, interfacing for the wavefront correction to the external DSM facility, part of the AOF[2][11].

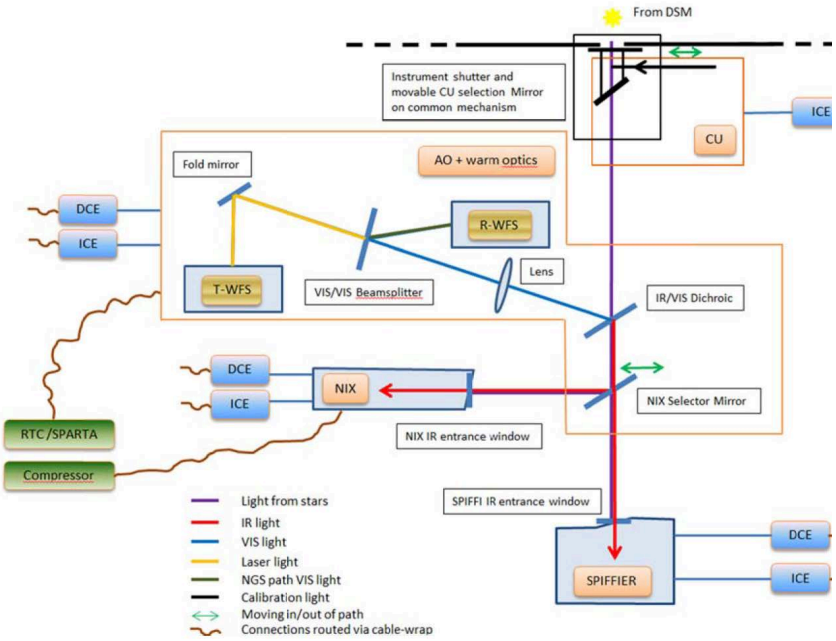

Figure 2 ERIS instrument scheme

The LGS-mode requires the implementation of two WFSs, the HO LGS WFS and the LO NGS WFS, requiring the introduction in the WO of a VIS/VIS Beam-Splitter in the optical branch reflected by the IR/VIS Dichroic. It separates the narrow-band Sodium LGS light from the rest of the visible radiation. Hereafter, we will refer to the VIS/VIS beam-splitter also as WFS Dichroic. The design joins the HO NGS functionality in the LO NGS WFS, separating the functionalities between the two WFSs in a purely on-axis LGS-dedicated WFS and an HO/LO NGS-dedicated WFS with off-axis capabilities. The LGS WFS is implemented in the beam transmitted through the WFS dichroic because the HO LGS loop is less sensitive with respect to the HO NGS loop to the astigmatism and chromaticity introduced by the transmission through the WFS dichroic substrate.

The AO WFSs opto-mechanical design has been constrained by the general design choice of using flat (or extremely slow) optics to relay the telescope beam to the AO WFSs to maximize the stability of Non Common Path Aberrations (NCPA). This is an opportunity, to be exploited, provided by telescopes with an adaptive secondary mirror, allowing to not introduce powered optics to integrate a DM in the AO module. As a direct consequence of this design choice, the selection of the NGS in the AO field is not performed by an optical field selector (tip-tilt mirror on a pupil image, requiring powered relay optics), but implementing each WFS units as a compact board supported by stages to scan the field (circular, about 32mm radius) and tracking the focus. This design choice is the standard approach for the AO systems developed by INAF-Arcetri for telescopes with Adaptive Secondary Mirrors and successfully experienced on LBT-FLAO[15] and Magellan-AO (MagAO)[16].

The mechanical scanning of the WFS board to patrol the field requires inserting a telecentric lens between the IR/VIS and VIS/VIS dichroic to relay the telescope exit pupil (M2) to infinity and keep the chief ray of the beam parallel regardless the off-axis. This is an extremely slow optics having the focal length equal to the distance to M2 (14.9 m), with extremely low sensitivity to misalignment.

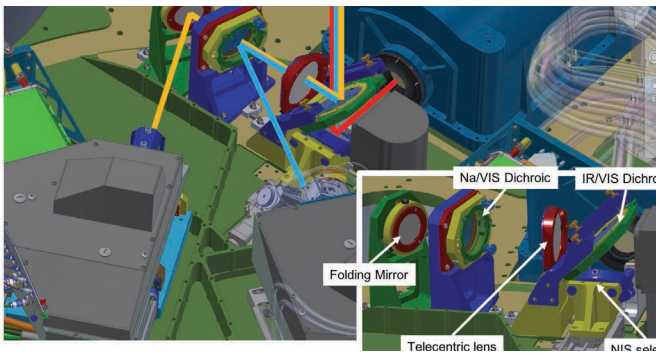

Figure 3. ERIS Warm Optics

The CU Selector Mirror is located upstream the IR/VIS Dichroic to allow the CU providing all the calibration needs to all the sub-systems. The size of the CUSM is driven by the NIX FoV and contributes to constraint the available space for the WO components. The distance between the Cassegrain Flange and the top of SPIFFIER provides another major space constraint to fit the WO design. That required to increase the Cassegrain Back Focal Length (BFL) by 250 mm with respect to the nominal VLT one, for a total of 500 mm from the Cassegrain rotator flange.

3. HO/LO NGS WFS UNIT

Figure 4 shows the design of the baseline NGS WFS implementation. It merges the HO and LO NGS WFS functionalities for the NGS and LGS mode, respectively. The HO configuration implements a 40x40 Shack-Hartmann (SH), i.e. the highest order compliant to the SPARTA/AOF and CCD220 format constraints. The LO configuration is implemented as a 4x4 SH array as a trade-off between pushing the performance toward the faint-end and allowing the sensing of a suitable number low orders modes for the truth sensing[4].

The main components and functions of the LO/HO WFS unit are:

1. A dual axis stage supporting the WFS board. One (focus) stage moves in the direction of the input optical axis, the other (X stage) in the orthogonal direction, parallel to the plane of the WFS board. The focus stage has a full stroke of 20 mm and is used to compensate for differential focus with respect to SPIFFIER and NIX, including drifts due to differential flexures and thermal expansion. The X stage, together with the periscope (see below), is used to patrol the NGS FoV (R=1' or R=32mm) and to compensate for all the effects introducing a differential image drift at the WFS focal plane with respect to the instrument focal plane. Part of the travel budget of the stages is used for the initial optical alignment of WO and WFS units to the ERIS reference axis.
2. A board, supported by the dual axis stage, where all the WFS components are mounted. The board can be separated from the stage for maintenance; the alignment is reproduced by pins between the board and the stage top plate.
3. A rotary stage supporting the Entrance Lens and a periscope. The axis offset of the periscope is 34 mm, allowing to patrol the full NGS FoV (R=32 mm) combining the periscope rotation with the X stage motion and some extra range (ΔR=2 mm) for alignment purposes. The periscope solution has been triggered by the vertical space constraints inside the ERIS central structure that does not allow implementing the vertical (Y) motion with a third stage.
4. The Entrance Lens produces a F/20 beam and relays the input telecentric focal plane to a tip-tilt mirror for pupil stabilization purposes (see below).
5. An ADC to compensate for PSF chromatic elongation due to atmospheric dispersion down to z=70deg allowing proper spatial filtering with the tunable field stop (see below) and avoiding sensitivity reduction for the SH in the LO configuration and for the acquisition camera.
6. A beam splitter dichroic transmitting wavelengths shorter than 600nm to the acquisition camera having 12arcsec diameter FoV. The wavelengths in the range 600nm-1000nm are reflected toward the pupil stabilization mirror.
7. The pupil stabilization mirror close to the F/20 focal plane used for stabilize the lateral decentering of the pupil on the SH lenslet array. The main contributors to the stroke requirement of the mirror are the pupil plane lateral drift due to alignment error between WFS and instrument rotator axis, PSF wobbling during K-prism rotation due to residual manufacturing and alignment errors, flexures and thermal effects, and possible telescope exit pupil shift.
8. The motorized iris diaphragm at the F/20 focal plane to implement a variable FoV stop, ranging from 2.5" to 0.8" diameter. The largest value corresponds to the maximum allowed FoV avoiding cross-talk among SH sub-apertures in HO mode. The minimum value, to be tuned during the AO verification and commissioning phase, is used to implement a spatial-filtered SH, similar to the one implemented in SPHERE and dedicated, in ERIS, to the coronagraphic observation modes and, in general, to on-

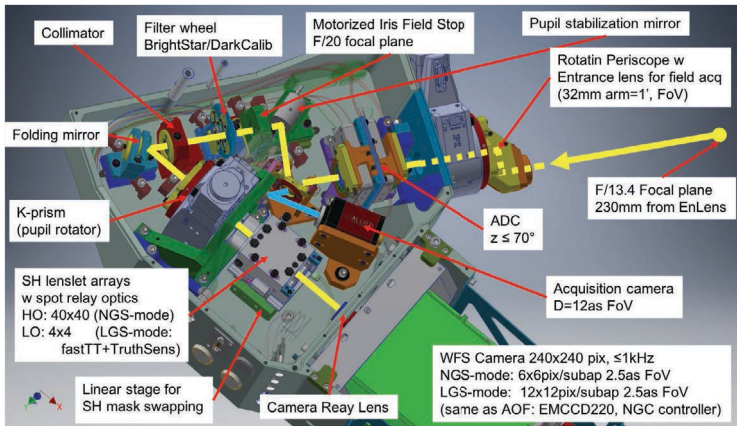

Figure 4. NGS WFS unit. The unit cover is removed to show the content.

axis pupil-tracking high contrast NGS-mode observations. The motorized field stop has been introduced during the Final Design Phase, after descoping the Pyramid WFS option[4] and retrieving part of its high contrast capabilities using the SH WFS.

9. A 4-stop filter wheel hosting a beam stop for dark calibration, a pass-all filter for normal operations and two filters to reduce the light level and avoid CCD220 over-illumination with bright NGSs (1<mR<2 and 1<mR<7 in the HO and LO configurations)
10. A collimator lens relaying an image of the pupil on the SH lenslet array.
11. A Pupil Rotator (named also K-prism), implemented with a reversion prism, to de-rotate the actuator pattern of the DSM on the SH lenslet array when ERIS instrument rotator is operating in field tracking mode.
12. A stage to switch between HO and LO SH lenslet arrays and related optics relaying the SH spots to the WFS Camera CCD. The HO and LO channels are implemented as two parallel barrels with a 40x40 and 4x4 SH arrays.
13. The ESO's WFS Camera (CCD220) having 240x240 pixel format. It is the same camera used for AOF, providing 6x6 pixel per subaperture in the HO configuration (2.5"/6=0.42"/pix). In the LO configuration the 2.5" FoV sampling is currently 12x12 pixel per subaperture (0.21"/pix).

4. LGS WFS UNIT

Figure 5 shows the design of the baseline LGS WFS implementation. The main components and functions are:

1. A focus stage supporting the WFS board. The stage is used for tracking the best focus of laser beacon when changing its distance with elevation and sodium profile evolution. The travel of the stage is also used for compensating differential focus positions with respect to SPIFFIER and NIX, including the focus drifts due to differential flexures and thermal expansion.
2. A board, supported by the focus stage, where all the WFS components are mounted. The board can be separated from the stage for maintenance; the alignment is reproduced by a set of mechanical references.
3. An Entrance Lens producing a F/20 beam and relaying the input focal plane to a tip-tilt mirror for pupil stabilization purposes.
4. A shutter to stop the incoming beam to protect CCD220 against over-illumination and calibrate dark frames.
5. A Pupil Rotator (the same as NGS WFS) to de-rotate the actuator pattern of the DSM on the SH lenslet array when ERIS instrument rotator is operating in field tracking mode.
6. The pupil stabilization mirror on the F/20 focal plane used for stabilize the lateral decentering of the pupil on the SH lenslet array. The main contributors to the stroke requirement of the mirror are the pupil plane lateral drift due to alignment error between WFS and instrument rotator axis, K-mirror and flexures. The mirror implements a mask for a 5.0" field stop to accommodate the elongated image of the sodium beacon.
7. A collimator lens relaying an image of the pupil on the SH lenslet array.
8. The ESO's WFS Camera (CCD220) including an internal 40x40 lenslet array with the same size of the CCD (5.76 mm). It is the same camera and SH array used for AOF, providing 6x6 pixel per subaperture with a FoV of 5".

The LGS WFS operates only on-axis, therefore it does not require stages to patrol the field. LGS on-axis location and stabilization are devoted to the 4LGSF launcher, providing an internal large stroke field steering mirror for LGS acquisition and drift tracking, and a low stroke fast TT corrector.

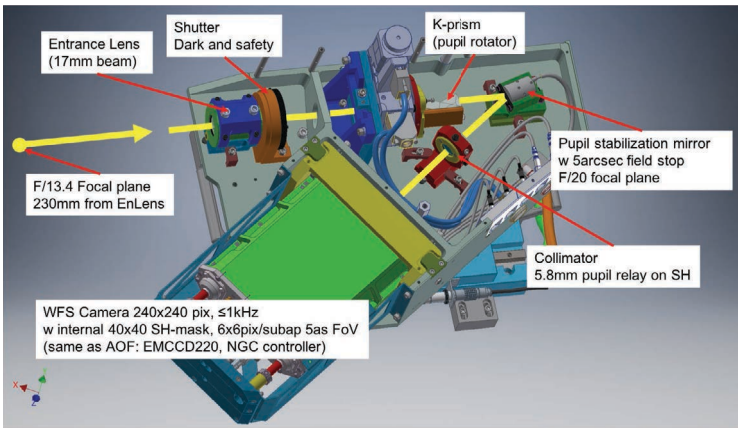

Figure 5. NGS WFS unit. The unit cover is removed to show the content.

5. AO SYSTEM PERFORMANCE

The ERIS AO system performance is computed in terms of Strehl ratio (SR) as a function of the NGS magnitude and it is shown in Figure 6 for the Ks band in comparison with the top-level requirements for both LGS and NGS modes. The curves have been obtained adding to the end-to-end numerical simulation results the wavefront error budget components that have not been directly included in the simulation. A

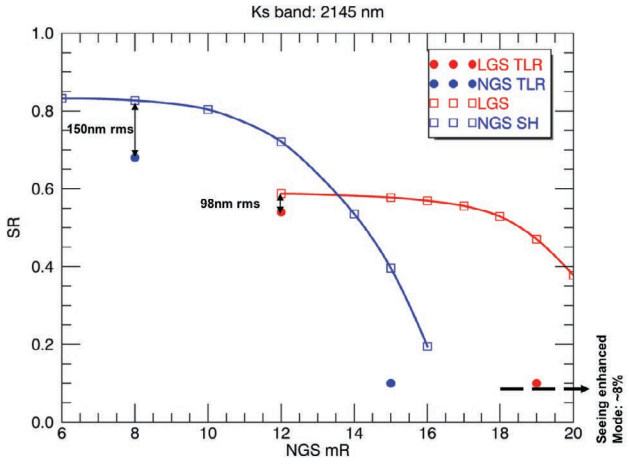

Table 1. Main simulation parameters

Seeing	0.87 arcsec (at z=30°)
WFS camera	EMCCD 240x240 pix
HO/LO NGS subap FoV wavelengtl Pix/subap	SH; HO:4x4 subap; LO:4x4 s 2.5 arcsec λ_{eff} = 768 nm (BW=600-100 HO: 6x6; LO: 12x12

subset of parameters of tl numerical simulation are shown Table 1. The complete set simulation parameters and description of the error budg components are reported Ref. [4].

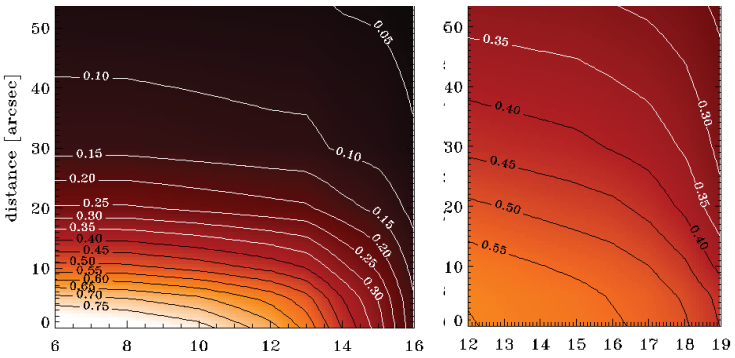

The contributions of the err budget in addition to the end-t end simulation are 112 nm ar 144 nm rms WFE for the NGS ar LGS modes respectively. They a dominated by an extreme conservative contribution of tl residual vibration compensation of 83 nm and 109 nm rms, based on vibration data taken with SINFONI at the Cassegrain focal station of VLT. The simulations does not consider the effect of the Active Vibration Cancellation algorithm developed by ESO[17].

For each NGS magnitude, both in NGS and LGS mode, the number of correcting modes and related loop gains, the loop frequency, the Gaussian size of the WCoG weighting maps and the CCD220 gain have been optimized.

The performance shows a conservative SR(Ks)=82% in the on-axis bright end in NGS mode and 59% in LGS mode. For on-axis observations, the NGS magnitude for selecting the better performing mode (LGS/NGS) is m_R=13.2 (transition magnitude). The comparison with the TLR requirements shows a contingency of 150nm and 98nm rms WFE in the bright end of the NGS (m_R=8) and LGS (m_R=12) mode, respectively.

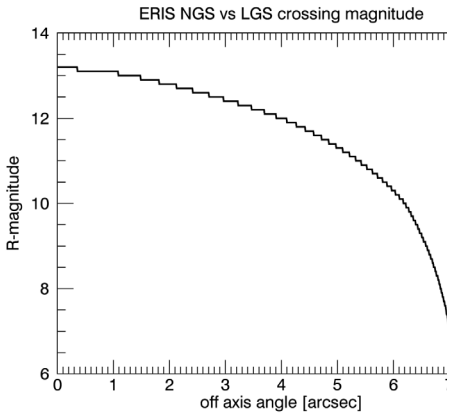

Figure 8 Transition magnitude vs NGS off-axis angle. Below the curve NGS-mode performs better than LGS-mode; the opposite above the curve.

Figure 10. One of the two WFS cameras and the related electronics in Arcetri (provided by ESO)

Figure 7 shows the off-axis behavior of NGS and LGS performance. Due to the faster degradation of performance with off-axis angle in the NGS-mode due to the different source of anisoplanatism error for NGS and LGS (high-order for the first and only tilt for the latter), the transition magnitude becomes brighter when increasing off-axis angle (see Figure 8) and LGS-mode observation are always more convenient, in terms of SR, for NGS off-axis larger than 7 arcsec, where the transition magnitude is mR~7.

6. MAIV STATUS

Integration of ERIS is made in two phases. In the first phase the sub-system are assembled and tested in the consortium partners premises: NIX at UK-ATC, SPIFFIER at MPE, CU at INAF-OAAb and AO at INAF-Arcetri. AO sub-system integration requires the ERIS main central structure, provided by MPE, and scheduled to be shipped to Arcetri at mid-July. Figure 9 shows the brand new 9m x 5m integration hall in INAF-Arcetri providing a 5ton double-hook crane and all the needed utilities, waiting for ERIS central structure.

In the second integration phase, the sub-systems, after local acceptance, will be shipped to MPE in springtime 2019, for the full instrument integration, test, and final acceptance before the shipping to Paranal beginning of 2020.

RTC and WFS Cameras

WFS cameras and SPARTA RTC (see Figure 10) has been delivered to INAF-Arcetri from ESO, including the ERIS specific firmware and software, like the truth sensing implementation and the modal NCPA application. For a more detailed description of the real-time and auxiliary loops handled by SPARTA, refer to [4].

Electronics and motion devices

The control electronics and motion devices have been all procured and tested. As an example, Figure 11-left shows the test under gravity full load of the WFS support boards and Figure 12 shows the cold test of the motion devices in the functional range [-10°C, +25°C]. Particular care has been taken for the design and test of WFS support stages because NGS WFS represents the pointing reference in both LGS- and NGS-modes, requiring high stiffness to keep under control differential flexures with respect to the science instruments. This requirement fc

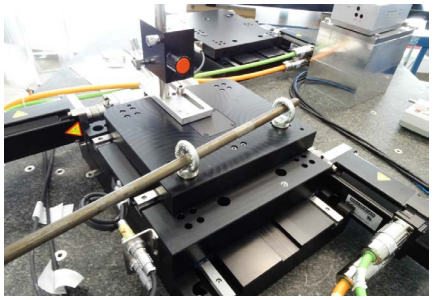

Figure 11. NGS WFS stage under vertical full-load test (Left) and under interferometric flexure testing (Right) during the acceptance test in Steinmeyer GmbH premises.

Figure 12. Cold test of motion devices

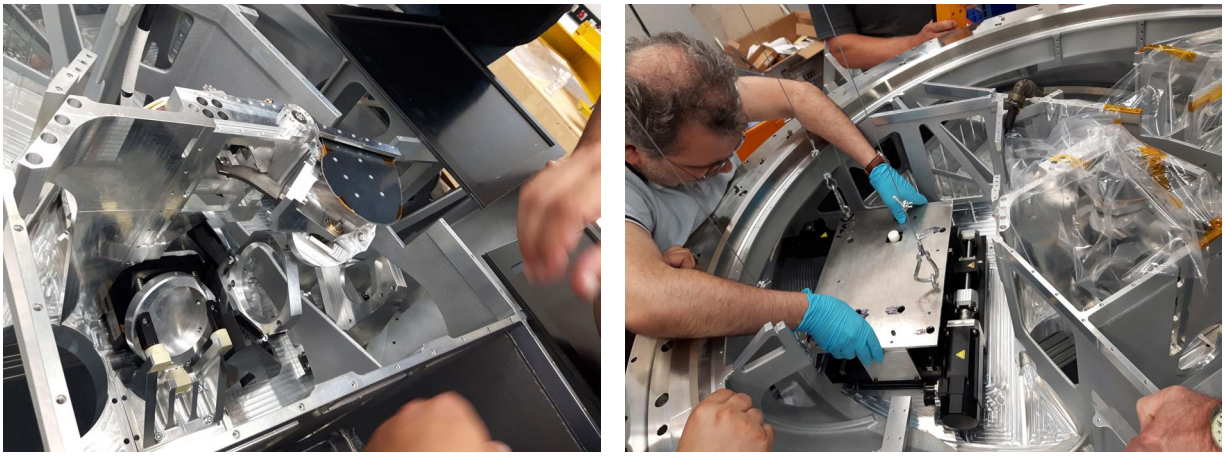

Figure 13. Fit and interface check of the Warm optics (left) and WFS boards (right) in the ERIS central structure.

stages (by Steinmeyer GmbH) that resulted in a production of stages in agreement with specification, as verified with extensive laboratory tests (see Figure 11-right for an example).

Because the DSM is not available for the ERIS AO acceptance tests in Europe, closed loop AO functionality will be tested using an ALPAO DM. A dedicated custom interface electronics between SPARTA and ALPAO is available to provide the same DSM interface for SPARTA in order to run the AO system without changes at the RTC interface level (see Figure 14). The interface electronics has been provided by Microgare srl, the same company providing DSM electronics.

Mechanics

Most of the mechanics has been manufactured and is currently in assembly phase. Pre-assembled mechanics has been used for an early check of the fitting and an interface test with the main instrument structure (Figure 13) as risk mitigation action, before shipping the structure in Arcetri.

Warm Optics and WFSs mechanics final assembly, including the related motion devices, is scheduled for the end of July.

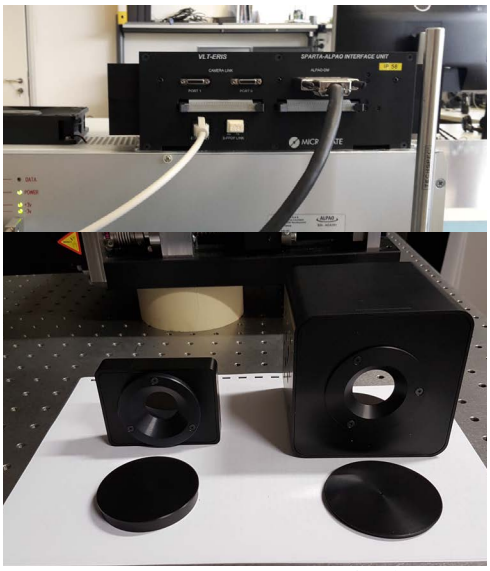

Figure 14 Bottom: ALPAO mirrors for the DSM simulator. Top: ALPAO-SPARTA custom interface electronics (by Microgate sl)

Optics

Optics are currently in manufacturing phase. WFS optics will be delivered to INAF-Arcetri at the end of July to be integrated with WFS mechanics and start the internal optical alignment. The light sources for the alignment (providing the correct F-number and entrance pupil size and location) are already available and tested (see Figure 15).

IR/VIS dichroic requires a longer procurement time, and will be substituted with a mirror during the AO test in Arcetri, where no IR

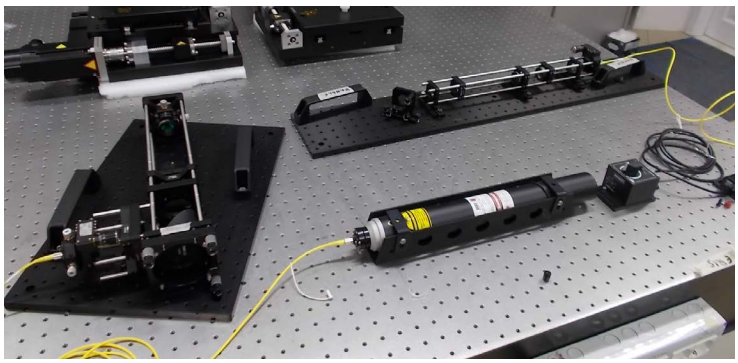

Figure 15 Alignment source for the NGS and LGS WFS

science instruments are present (they will be integrated at MPE for the full ERIS acceptance, as described at the beginning of the present section).

7. CONCLUSIONS

The ERIS Consortium successfully passed the Final Design Review end of May 2017 and now the project is in the Manufacturing and Assembly Phase.

The ERIS AO system design makes a large re-use of AOF technology to save development and implementation time: the Deformable Secondary Mirror, the 4LGS Facility, the WFS Cameras (EMCCD) and the SPARTA RTC.

The required observing modes (LGS, NGS and Seeing Enhanced) are implemented with the use of two SH WFSs units. The on-axis LGS-only WFS board implements the 40x40 SH with 5as FoV and is located on a linear stage for Na layer tracking. The NGS-only WFS is able to switch between a HO (40x40 SH, 2.5as FoV) and a LO (4x4 SH, 2.5as FoV) configuration for the NGS and the LGS mode respectively. The LO configuration provides also the truth sensing function for the LGS WFS focus and slope offset tuning. The NGS WFS board is located on a dual-axis stage to patrol the R=1arcmin acquisition field (together with the on-board periscope) and the compensation of the differential focus with respect to the science instruments.

The numerical simulations and analysis show that the SR requirements required by the TLRs are met with a contingency of 150nm and 98nm rms WFE in the bright end of the NGS (m_R=8) and LGS (m_R=12) mode, respectively.

The AO module is currently in assembly phase: the motion devices and electronics have been already procured and assembled, allowing the functionality test and control optimization of the devices. Mechanics is proceeding with final assembly. Mechanics pre-assembly has been performed for an early fit and interface check. Optics is in manufacturing phase. Delivery of the WFS optics is scheduled for the end of July. Optical alignment tools are ready to proceed with the WFS assembly.

The AO sub-systems, after local acceptance, will be shipped to MPE in springtime 2019, for the full instrument integration, test, and final acceptance before the shipping to Paranal beginning of 2020.

8. ACKNOWLEDGMENTS

The ERIS AO team thanks the staff at the partner institutes, at ESO in Garching, and at ESO Paranal, for continued support and enthusiasm for the project.

REFERENCES

[1] Davies, R., *et al.* “ERIS: revitalising an adaptive optics instrument for the VLT,” Proc SPIE 10703 (2018).
[2] Madec, P.-Y., *et al.* “Adaptive Optics Facility: from an amazing present to a brilliant future,” Proc. SPIE 10703 (2018).
[3] Oberti, S., *et al.* “The AO in AOF,” Proc. SPIE 10703 (2018).
[4] Riccardi, A., *et al.* “The ERIS Adaptive Optics System.” Proc SPIE 9909, p. 99091B (2016).
[5] Taylor, W. D., *et al.* “NIX, the imager for ERIS: the AO instrument for the VLT,” Proc. SPIE 9909, p. 99083F (2016).
[6] Glauser, A. M., *et al.* “Development of cryogenic mechanisms for the VLT/ERIS instrument.” Proc SPIE 10702 (2018).
[7] Boehle, A., *et al.* “Cryogenic characterization of the grating vector APP coronagraph for the upcoming ERIS instrument at the VLT.” Proc SPIE 10702 (2018).
[8] Kenworthy, M. K., *et al.* “High contrast imaging for the enhanced resolution imager and spectrometer (ERIS).” Proc SPIE 10702 (2018).
[9] George, E. M., *et al.* “Making SPIFFI SPIFFIER: upgrade of the SPIFFI instrument for use in ERIS and performance analysis from re-commissioning,” Proc SPIE 9909, p. 99080G (2016).
[10] Dolci, M., Di Rico, G., Valentini, A., Di Cianno, A., “Final design and construction of the ERIS calibration unit,” Proc SPIE 10702 (2018).

[11] Briguglio, R., Biasi, R., Xompero, M., Riccardi, A., Andrighettoni, M., Pescoller, D., Angerer, G., Gallieni, D., Vernet, E., Kolb, J., Arsenault, R., Madec, P.-Y., "The deformable secondary mirror of VLT: final electro-mechanical and optical acceptance test results," Proc. SPIE 9148, p. 914845 (2014).
[12] Hackenberg, W. K., *et al.* "ESO 4LGSF: Integration in the VLT, Commissioning and on-sky results," Proc SPIE 9909 (2016).
[13] Di Rico, G., "Control electronics of the ERIS AO and CU subsystems," Proc. SPIE 10703 (2018).
[14] Baruffolo, A., Salasnich, B., "Design of the ERIS instrument control software," Proc. SPIE 10707 (2018).
[15] Esposito, S., Riccardi, A., Pinna, E., Puglisi, A., Quiros-Pacheco, F., Arcidiacono, C., Xompero, M, Briguglio, R., Agapito, G., Busoni, L, Fini, L., Argomedo, J, Gherardi, A, Brusa, G., Miller, D., Guerra, J. C., Stefanini, P., Salinari, P., "Large Binocular Telescope adaptive optics system: new achievements and perspectives in adaptive optics," Proc. SPIE 8149, p. 814902 (2011).
[16] Close, L. M., Males, J. R., Morzinski, K. M., "MagAO status and visible light science," Proc. SPIE 10703 (2018).
[17] Muradore, R., Pettazzi, L., Fedrigo, E., Clare, R., "On the rejection of vibrations in Adaptive Optics Systems," Proc. SPIE 8447, p. 844712 (2012).